The effective mass and Landé factor of the degenerate electron gas

2000 J. Phys.: Condens. Matter 12 2007

(http://iopscience.iop.org/0953-8984/12/9/305)

J. Phys.: Condens. Matter **12** (2000) 2007–2020. Printed in the UK PII: S0953-8984(00)07835-8

The effective mass and Landé factor of the degenerate electron gas

H M Böhm and K Schörkhuber
Institut für Theoretische Physik, Johannes Kepler Universität, A-4040 Linz, Austria

Received 15 September 1999

Abstract. We study the effective mass and the Landé factor for the three-dimensional as well as the two-dimensional degenerate electron gas. The influences of specific approximations to the self-energy and the vertex, equivalently formulated in terms of static and local effective interactions, are examined, with the aim of developing a legitimate and straightforward description of realistic low-dimensional semiconductor structures. The results obtained are tested against reference data from the literature. We further apply the formalism to a $Si–SiO_2$ metal oxide–semiconductor (MOS) structure and compare the predictions with experiment.

1. Introduction

For the interacting electron gas, recent years have seen substantial progress as regards deriving highly reliable results from simulations of its response to static external modulations [1–3]. From these a localized effective particle–hole interaction can be extracted. Also, the results on fundamental properties have been supplemented by ones from updated simulations involving refined techniques [4–6].

These most accurate results, however, are restricted to three-dimensional (3D) and two-dimensional (2D) jellium. The description of more realistic systems such as heterostructures and inversion layers still relies on more elementary approaches such as generalizations of the random-phase approximation (RPA).

The purpose of this work is to investigate the use of such reasonably simple theoretical models for calculating two important observables, the effective mass m^* and the effective Landé factor g^*, to compare the results with those obtained on the basis of published Monte Carlo (MC) data, and to test them against highly accurate results available in the literature [5,7]. Furthermore, we apply the formalism to a quasi-2D MOSFET structure in order to compare the results with experimental data.

Much progress concerning the effective mass in 3D has been made with the use of effective interactions [8–13] (different approaches are found in references [14, 15]). For 2D and quasi-2D systems, experiments [16–18] on inversion layers inspired various investigations [19–24]. Calculations for a GaAs heterostructure [25] and for the strictly 2D system were also published [26].

In section 2 we discuss the results obtainable with the simplest diagram for the self-energy, and use *state-of-the-art* descriptions of the dielectric function in section 3. In section 4 the irreducible particle–hole interaction is better accounted for, and the significance of the localization procedure is investigated in section 5. Next, spin effects are included and two routes for modelling the effective interaction are examined (section 6). Section 7 gives a

0953-8984/00/092007+14$30.00

critical comparison of the two models. Finally, the application to a realistic MOSFET layer is presented in section 8.

2. Basic relations

The influence of the Coulomb interaction

$$v(k) = \begin{cases} 4\pi e^2/k^2 & D = 3 \\ 2\pi e^2/k & D = 2 \end{cases} \tag{1}$$

on an electron's effective mass is commonly obtained from the poles of the single-particle propagator G_σ, defining the quasi-particle excitations E_k. With use of the system's self-energy Σ_σ (σ is the spin), one obtains for the relation of the bare mass m to the effective mass

$$\frac{m}{m^*_{\mathrm{Ek}}} = \left.\frac{1 + (m/k)(\partial/\partial k)\Sigma_\sigma(k,\omega)}{1 - (\partial/\partial\omega)\Sigma_\sigma(k,\omega)}\right|_{k=k_\mathrm{F},\omega=E_k=\varepsilon_\mathrm{F}} \tag{2}$$

(where k_F and ε_F denote the Fermi momentum and energy; the usual density parameter r_s is introduced as $\alpha r_s = k_\mathrm{F} a_\mathrm{B}$, with a_B denoting Bohr's radius and $\alpha = (4/9\pi)^{1/3}$ in 3D and $1/\sqrt{2}$ in 2D). Also frequently used is the so-called 'on-shell' approximation:

$$\frac{m}{m^*_{\mathrm{os}}} = \left[1 + \frac{m}{k}\frac{\partial}{\partial k}\Sigma_\sigma(k,\omega) + \frac{\partial}{\partial\omega}\Sigma_\sigma(k,\omega)\right]_{k=k_\mathrm{F},\omega=\varepsilon_\mathrm{F}}. \tag{3}$$

In diagrammatic language, Σ_σ can be expressed in terms of G_σ, the effective interaction $v(k)/\epsilon(k,\omega)$ (where ϵ is the dielectric function), and the proper vertex Γ. The latter is the solution of an integral equation given by

$$\Gamma(\boldsymbol{k},\omega;\boldsymbol{q},\varepsilon) \equiv 1 + \sum_{\sigma'}\int\frac{\mathrm{d}^D\boldsymbol{k}'}{(2\pi)^D}\int\frac{\mathrm{d}\omega'}{2\pi\mathrm{i}}\,G_{\sigma'}(\boldsymbol{k}-\boldsymbol{k}',\omega-\omega')G_{\sigma'}(\boldsymbol{k}',\omega') \\ \tilde{I}_{\sigma\sigma'}(\boldsymbol{k},\omega,\boldsymbol{k}',\omega';\boldsymbol{q},\varepsilon)\Gamma(\boldsymbol{k}',\omega';\boldsymbol{q},\varepsilon). \tag{4}$$

The kernel $\tilde{I}_{\sigma\sigma'}$ is by definition *irreducible* in the *particle–hole* channel.

The simplest approach is to replace $\tilde{I}_{\sigma\sigma'}$ by zero. This results in a closed set of equations that can be solved self-consistently, and is known as the GW-approximation. Most authors, however, additionally replace the interacting propagator G_σ by its free counterpart G^0, and we prefer to clearly indicate this by denoting the approximation as 'G^0W'. The self-energy is then obtained from its RPA expression:

$$\Sigma(\boldsymbol{k},\omega) = -\int\frac{\mathrm{d}^D\boldsymbol{k}'}{(2\pi)^D}\int\frac{\mathrm{d}\omega'}{2\pi\mathrm{i}}\,\frac{v(k')}{\epsilon(k',\omega')}G^0(\boldsymbol{k}-\boldsymbol{k}',\omega-\omega') \tag{5}$$

where $\epsilon = 1 - v\Pi^0$ is the Lindhard dielectric function [27, 28]. By Wick's rotation, the frequency integral can be transformed into two parts, a residual one and a line contribution. The residual part is given by a one-dimensional integral that is determined by the *dielectric function at zero frequency*. For the second part there remain two double integrals which are determined by *the dielectric function on the imaginary axis*.

A straightforward improvement of the RPA calculation of m^* is achieved by including a so-called 'local field correction' $\mathcal{G}_+$ in the dielectric function in equation (5):

$$\epsilon(k,\omega) = 1 - \frac{v(k)\Pi^0(k,\omega)}{1 + v(k)\mathcal{G}_+\Pi^0(k,\omega)}. \tag{6}$$

Here, the product $v\mathcal{G}_+$ can be understood as a local approximation for the effective particle–hole interaction $\tilde{I}$ appearing in equation (4). $\mathcal{G}_+$ is conveniently modelled in a modified Hubbard form [29], which reads (measuring all wave vectors in k_F)

$$\mathcal{G}_+(k) = \frac{Ak^{D-1}}{2[k^2 + AB]^{(D-1)/2}}. \tag{7}$$

The coefficients A, B are fixed according to various limiting conditions ('sum rules'). The choice $A = 1$, $B = 1 + (q_{TF}/k_F)^{D-1}$ with q_{TF} denoting the Thomas–Fermi wave vector [30] was suggested by Rice [31]—in order to improve fulfilment of the compressibility sum rule.

Practically *any* result between the RPA and Hubbard ones can be obtained by suitable choices of A, B. Hence for a meaningful calculation of m^* it is important to decide on appropriate criteria. The integrand of the residual part is restricted to $q \leqslant 2k_F$ and governed by the $\omega = 0$ behaviour. Certainly, a proper treatment of the compressibility sum rule

$$\mathcal{G}_+(k \to 0, \omega = 0) \stackrel{!}{=} \left(\frac{k}{q_{TF}}\right)^{D-1} \left(1 - \frac{\kappa^0}{\kappa}\right) \tag{8}$$

(where $\kappa^{(0)}$ denotes the (free) isothermal compressibility of the system) is crucial for this term.

The integrand of the line contribution vanishes rapidly for large q. At $2k_F$ there is an integrable singularity, where positive and negative contributions mutually cancel. The important range of wave vectors thus is again the region $q \approx 0$–$1.5\ k_F$. Therefore an inappropriate treatment of equation (8) can be expected to lead to sizable errors for this term also (though we are not aware of any sum rule for imaginary frequencies). We note, in particular, that Rice's approach [31] does *not* fulfil this sum rule (κ is already off by more than 10% for $r_s \geqslant 3.5$ (2.5) in the 3D (2D) case).

The short-range repulsion of the Coulomb interaction leads to the Kimball relation [32,33]

$$\mathcal{G}_+(k \to \infty) \stackrel{!}{=} 1 - g(0) \tag{9}$$

where $g(0)$ is the pair distribution function at zero distance. This requirement is different from the condition for the static part of a *dynamic* local field correction [34]:

$$\mathcal{G}_+(k \to \infty, \omega = 0) \stackrel{!}{=} \frac{-2}{\rho v(k)} \Delta\varepsilon_{kin} + \left\{ \begin{array}{ll} 2/3 & (D = 3) \\ 1 & (D = 2) \end{array} \right\} (1 - g(0)) + \mathcal{O}(k^0) \tag{10}$$

where $\Delta\varepsilon_{kin}$ denotes the difference between the interacting and free kinetic energies per particle and ρ is the density. It is seen that here $\mathcal{G}_+$ diverges proportionally to k^{D-1}.

The rhs of equations (8), (9) evaluated from MC data for the correlation energy [35, 36] and ladder summation results for $g(0)$ [37, 38] (denoted by 'Co + K') is used to fix A and B.

A final word is in order concerning the comparison between on-shell and renormalized 'Ek' mass. Yasuhara and Takada [12] argue that if $\Sigma_\sigma(\boldsymbol{k}, \omega; [G])$ is known as a functional of G^0 (instead of G), the first iterative solution is superior to a self-consistent treatment using the *same* functional form. We depict both m^*_{os} and m^*_{Ek} in figure 1 for our modified Hubbard approach and the two 'bounding' RPA and plain Hubbard results. It is seen that the curves for the 'Ek' masses develop a decreasing slope, whereas the on-shell results rise steeply; they are found to diverge for $r_s = 17$ (60) for the 3D jellium within the Hubbard approximation (RPA), and for $r_s = 5$ (20) in 2D (again, within the Hubbard approximation (RPA)). Whereas in the 3D case this may still provide a reasonable description for the metallic density range, it is unacceptable for 2D, where r_s-values of 20 can be obtained by doping and the application of gate voltages. Consequently (and although neither m^*_{os} nor m^*_{Ek} is conceptually superior), we present most results for the case of m^*_{Ek}.

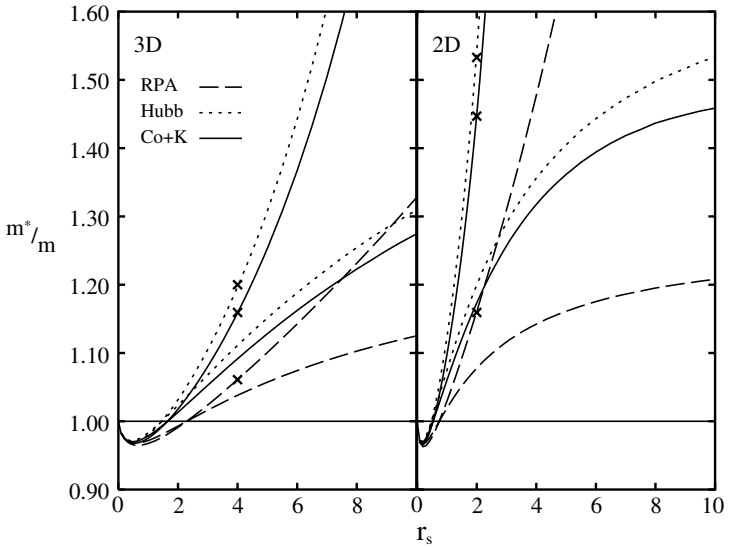

Figure 1. Comparison between the on-shell and 'Ek' effective mass for the 3D (left) and 2D (right) electron gas. The RPA, Hubbard approximation, and modified Hubbard approximation are given by the long-dashed, short-dashed, and solid lines, respectively. The on-shell results are marked by crosses (×). In all four cases the RPA and Hubbard data bracket those of the modified approach.

3. G^0W-description based on Monte Carlo results

In order to test the suitability of a local field of the specific analytic form (7) (excluding e.g. any possible peak structure of $\mathcal{G}_+$), we propose to use *state-of-the-art local field corrections* obtained from MC simulations.

Moroni *et al* [2] calculated the static response of 3D jellium to a periodic external potential for $r_s = 2, \ldots, 10$ by diffusion MC studies and thus obtained precise results for $\mathcal{G}_+(k, \omega = 0) \equiv \mathcal{G}_+^{\mathrm{MCS}}(k)$. They found that this quantity is almost completely given by its asymptotes, i.e. by equation (8) and the k^2-term of equation (10). They have also determined $1/\epsilon(k, 0) - 1$ for the 2D system [1]. Again, their data can be well reproduced by using equations (8) and (10) for $\mathcal{G}_+$. We have tested that for the 3D system this piecewise-linear approximation of $v\mathcal{G}_+$ versus k^{D-1} yields only marginal differences for m^* in comparison with the fit of reference [2]. Accordingly, this approximation can be trusted for 2D. The integrand of the residual part is thus very well known.

The calculation of the static structure factor $S(k)$ via the fluctuation-dissipation theorem is best performed along the imaginary axis:

$$S(k) = -\int_0^\infty \frac{\mathrm{d}\varepsilon}{\rho\pi}\, \Im\left[\frac{\Pi^0(k, \mathrm{i}\varepsilon)}{1 - v(k)[1 - \mathcal{G}_+]\Pi^0(k, \mathrm{i}\varepsilon)}\right] \tag{11}$$

involving thus an 'overall treatment' of the frequency dependence of $\mathcal{G}_+$ analogous to that of the line term. Since $S(k)$ is well known from simulation studies [4, 6], we propose to use equation (11) as an alternative for determining the static function $\mathcal{G}_+^{\mathrm{SFD}}(k)$. In the actual computation we have taken $S(k)$ from the Fourier transform of the fit of reference [4] for the 3D case, and from references [6] and [39] for 2D. Unfortunately, for $k \to 0$ (inaccessible to MC study) these data have rather large statistical uncertainties. Therefore we smoothly interpolated between the simulated data for $k \gtrsim k_{\mathrm{F}}$ and the small-k behaviour on the basis of the compressibility sum rule (though, however, $S(k \to 0)$ is mostly determined by the

plasmon dispersion, which is again not exactly known). Improved MC data at (moderately) *long* wavelengths would thus be highly desirable.

Thus we now have two static local fields of high quality. For $k \to \infty$, equation (11) implies the behaviour (9) in contrast to the k^{D-1}-divergence of the MCS results. This leads to a discrepancy for the data in the intermediate-k regime, reflecting the limitations of a frequency-independent approach for $\mathcal{G}_+$. Noticeable differences between the two MC-based quantities with the modified Hubbard function are already appearing at around $k \approx 1\ k_F$, a value well inside the region important for the integration.

The effective masses obtained with both local field corrections are displayed in figure 2 in comparison with the prediction from the modified Hubbard approach. Additionally shown are reference results from the literature. The 3D values that we use were obtained from the summation of ring and ladder diagrams in the 'correlated-basis-function' formalism [7]; the 2D m^* was directly obtained in MC studies [5]. The rise of both data with r_s is considerably less steep. Compared to this trend, the deviations of the SFD and MCS data from the modified Hubbard data are of little significance.

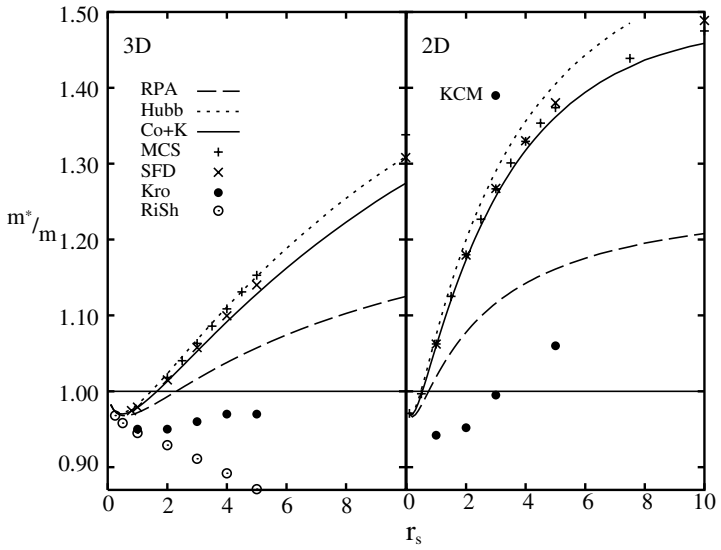

Figure 2. The effective mass in the G^0W-approach for the state-of-the-art local field corrections. The SFD results based on $S(k)$ are marked by crosses ($\times$), those obtained using the $\omega = 0$ MCS data by + symbols. As before, the RPA, Hubbard, and modified Hubbard results are given by the long-dashed, short-dashed, and solid lines, respectively. The full circles are the results of Krotscheck [7] for the 3D case and those of Kwon *et al* [5] for the 2D case. The open circles are the data from reference [40].

We include in figure 2 the data given by Rietschel and Sham [40], who determined m^* in the RPA fully self-consistently. It is seen that their data decrease with r_s and lie much lower than the reference values (like the self-consistent data of reference [14]). Accounting for self-energy insertions thus does not lead to satisfactory results, and two conclusions can be drawn:

(i) The G^0W-approach, even with the most accurate $\mathcal{G}_+$, *cannot* describe the effective mass satisfactorily. The inclusion of vertex insertions is crucial.

(ii) Given the assumption of the formal dependence of Σ_σ on $\mathcal{G}_+$, studies based on a modified Hubbard approximation provide a good estimate of the resulting m^*, since the basic

trend of the r_s-dependence is the same as for the most sophisticated local fields. This is important for applications to realistic low-dimensional systems, where no simulation data are available.

4. Effective interaction

The self-energy and the single-particle propagator are connected by the ($\boldsymbol{q} \to \boldsymbol{0}, \varepsilon \to 0$) limit of *exactly* the same function $\tilde{I}_{\sigma\sigma'}$ that determines the vertex in equation (4). Vignale and Singwi [9] proposed a *static and local* approximation, $\tilde{I}_{\sigma\sigma'}(|\boldsymbol{k}-\boldsymbol{k}'|)$, that, together with certain assumptions concerning the classes of diagrams retained, allows a straightforward calculation of Σ_σ and thus of the effective mass [10]. A thorough discussion was later given by Yasuhara and co-workers [12, 13]. The result is very similar to a G^0W-expression, equation (5), but with v/ϵ replaced by the average effective *particle–particle* interaction $V^{\mathrm{eff}} = [V_{\uparrow\uparrow} + V_{\uparrow\downarrow}]/2$ with [9]

$$V^{\mathrm{eff}}(k,\omega) = v(k) + \{v(k)[1-\mathcal{G}_+(k)]\}^2 \frac{\Pi^0(k,\omega)}{1 - v(k)[1-\mathcal{G}_+(k)]\Pi^0(k,\omega)}. \tag{12}$$

This quantity was first introduced by Overhauser (see [8]), who pointed out that for electrons with like spins the effective interaction $V_{\uparrow\uparrow}$ is intrinsically different from the one for particles with opposite spins, $V_{\uparrow\downarrow}$.

$\mathcal{G}_+$ is identical to the symmetric part of the localized irreducible particle–hole interaction:

$$v(k)\mathcal{G}_\pm(k) \equiv \frac{1}{2}[\tilde{I}_{\uparrow\uparrow}(k) \pm \tilde{I}_{\uparrow\downarrow}(k)] \equiv \frac{1}{2}v(k)[\mathcal{G}_{\uparrow\uparrow}(k) \pm \mathcal{G}_{\uparrow\downarrow}(k)] \tag{13}$$

and the approximations for $\tilde{I}_{\sigma\sigma'}$ that lead to equation (12) differ from the mere inclusion of $\mathcal{G}_+$ in Γ as introduced by Rice [31] (and applied in 2D in references [19, 25]). As in section 3, we use the modified Hubbard form fulfilling equations (8), (9), as well as the two most refined local fields constructed from available MC data. The results for m^*_{Ek} (cf. figure 3) now obviously

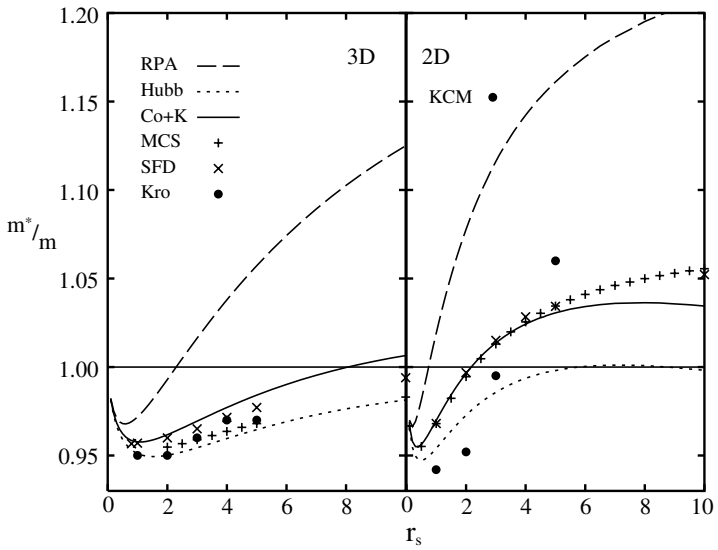

Figure 3. The effective mass m^*_{Ek} without spin fluctuations. The notation is the same as for figure 2.

reproduce the right trend as a function of r_s. (This is *not* the case if $\mathcal{G}_+$ is included in Rice's way.) Properly accounting for all related diagrams for $\tilde{I}_{\sigma\sigma'}$ is thus crucial. Since $\mathcal{G}_+$ enters Σ in multiple ways, the 'order' of the curves is now reversed. Again it can be said that the modified Hubbard approximation yields a satisfactory description.

We finally note that $m^*_{\rm os}$ does not diverge at any value of r_s in the whole range that we investigated (up to $r_s = 80$ in 3D and 2D), indicating that the classes of diagrams are indeed chosen in a consistent manner. However, $m^*_{\rm os}$ is found to decrease for values of $r_s > 25$ (10) in 3D (2D). For the 'Ek' mass, this effect is much weaker.

5. Exchange contribution

The diagrams relevant for $\tilde{I}_{\sigma\sigma'}$ consist, to a significant extent, of exchange graphs. As such effects are *intrinsically non-local*, the question arises of whether a description based on the approximation $\tilde{I}_{\sigma\sigma'}(\boldsymbol{k}, \omega, \boldsymbol{k}', \omega'; \mathbf{0}, 0) \approx \tilde{I}_{\sigma\sigma'}(|\boldsymbol{k} - \boldsymbol{k}'|)$ is reasonable. We have therefore evaluated the leading exchange correction to the RPA on-shell mass (figure 4).

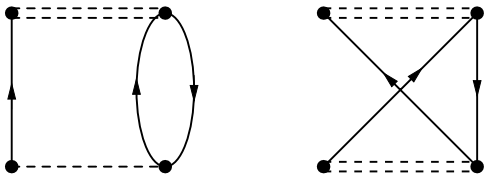

Figure 4. Leading diagrams of the self-energy. Left: $\Sigma_{\rm RPA}$. Right: the screened second-order exchange contribution. The single- and the double-dashed lines represent the bare and screened Coulomb interactions v and v/ϵ, respectively. The lines with arrows are free Green's functions.

This diagram can be transformed into a five-dimensional integral (a four-dimensional one in 2D), which is evaluated numerically. The result is added to the RPA term, the corresponding sum being shown in figure 5. For comparison we depict the *same* contribution in the Hubbard approximation (with appropriately corrected prefactors [13]).

The inclusion of exchange gives a significant deviation from the RPA result; the Hubbard approximation is noticeably different, but not too far from the non-local result. This shows that to the order of v^2 the localization gives a good answer for the effective mass. Consistently with the direct contribution, we have estimated the screening by using $v(k)/\epsilon^{\rm RPA}(k, \omega)$. As is to be expected, this diminishes the exchange contribution, which nevertheless remains rather large. Compared to the influence of screening, that of the localization is less important. Therefore the summation of large classes of diagrams with the help of local field corrections provides a reasonable working basis.

6. Inclusion of spin fluctuations

The inclusion of spin fluctuations was first studied by Ng and Singwi [10] and has been thoroughly discussed by Giuliani's group [24]. The self-energy can again be cast into the form (5), with the effective potential [10, 11]

$$V^{\rm eff} = v + \{v[1 - \mathcal{G}_+]\}^2 \frac{\Pi^0}{1 - v[1 - \mathcal{G}_+]\Pi^0} + 3\{v[\mathcal{G}_-]\}^2 \frac{\Pi^0}{1 + v\mathcal{G}_-\Pi^0}. \qquad (14)$$

To the best of our knowledge, no suitable MC data are available for the ω-integrated partial structure factors $S_{\uparrow\uparrow(\downarrow)}$ in 2D; for the $\omega = 0$ spin response function, simulation results [3] exist

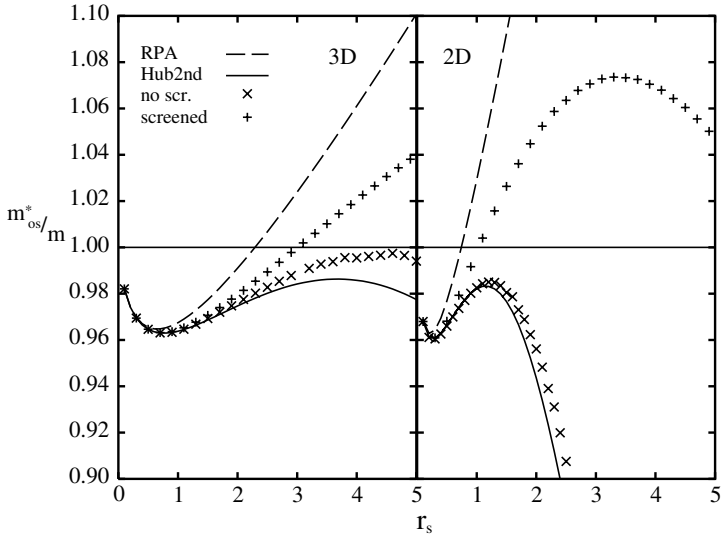

Figure 5. The on-shell effective mass obtained from the diagrams given in figure 4. The long-dashed line is the RPA without exchange; the results with the unscreened and the dynamically screened exchange effects included are given by the cross (×) and + symbols, respectively. The unscreened data should be compared with the leading-order Hubbard result (solid line).

only for $r_s = 2$. We therefore use a modified Hubbard description for both local field factors $\mathcal{G}_\pm$. The necessary sum rules for $\mathcal{G}_-$ are given as [41]

$$\mathcal{G}_-(k \to \infty) \stackrel{!}{=} g(0) \tag{15}$$

$$\mathcal{G}_-(k \to 0) \stackrel{!}{=} \left(\frac{k}{q_{\mathrm{TF}}}\right)^{D-1} \left(1 - \frac{\chi_{\mathrm{M}}^0}{\chi_{\mathrm{M}}}\right) \tag{16}$$

(the 'spin-stiffness sum rule'), where χ_{M} is the magnetic susceptibility, χ_{M}^0 its Pauli value. It can be obtained from the exchange–correlation energy per particle, $\varepsilon_{\mathrm{xc}}$, for which, however, its dependence on the relative magnetization ζ must be known:

$$1 - \frac{\chi_{\mathrm{M}}^0}{\chi_{\mathrm{M}}} = -\left\{\begin{array}{ll} 3/2 & (D=3) \\ 1 & (D=2) \end{array}\right\} (\alpha r_s)^2 \left.\frac{\partial^2 \varepsilon_{\mathrm{xc}}\,(\mathrm{Ryd})}{\partial \zeta^2}\right|_{\zeta=0}. \tag{17}$$

Finally, we note the identity [30]

$$\frac{\chi_{\mathrm{M}}}{\chi_{\mathrm{M}}^0} = \frac{m^*}{m}\frac{g^*}{g}. \tag{18}$$

It is important to note that the modified Hubbard approximation can now be incorporated in *two different ways*. The first is to assume the Hubbard form for the partial quantities in the spirit of Iwamoto and Pines [42, 43]

$$\mathcal{G}_{\uparrow\uparrow}^{\mathrm{IP}}(k) = \frac{A_{\uparrow\uparrow} k^{D-1}}{[k^2 + A_{\uparrow\uparrow} B_{\uparrow\uparrow}]^{(D-1)/2}} \tag{19}$$

and an analogous form for $\mathcal{G}_{\uparrow\downarrow}^{\mathrm{IP}}$. Alternatively, Yarlagadda and Giuliani suggest [23] applying the Hubbard form directly to $\mathcal{G}_\pm$:

$$\mathcal{G}_\pm^{\mathrm{YG}}(k) = \frac{A_\pm k^{D-1}}{2[k^2 + A_\pm B_\pm]^{(D-1)/2}}. \tag{20}$$

In both cases the parameters are fixed according to the sum rules (8), (9), (15), (16).

7. Landé factor

In the presence of an applied magnetic field H the quasi-particle energies for particles with different spins define the effective Landé factor g^*. From these, the Landau quasi-particle interaction function $f_{\sigma,\sigma'}(\boldsymbol{k}, \boldsymbol{q})$ can be obtained as a second functional derivative with respect to the momentum occupation function. For the case of a general G^0W-form (such as equation (5)) one obtains

$$f_{\sigma,\sigma'}(\boldsymbol{k}, \boldsymbol{q}) = -V^{\text{eff}}(\boldsymbol{k} - \boldsymbol{q}, \omega_k^0 - \omega_q^0)\delta_{\sigma,\sigma'} \tag{21}$$

where $\omega_k^0 = k^2/2m$ denotes the free-single-particle energies. The Landé factor can then be expressed as [30, 44]

$$\frac{g}{g^*} = 1 + \frac{m^*}{2\pi^2} \begin{cases} k_{\text{F}} \displaystyle\int_{-1}^{+1} \mathrm{d}\xi \; f_a(\xi) & \text{3D} \\ \displaystyle\int_0^{2\pi} \mathrm{d}\phi \; f_a(\cos\phi) & \text{2D} \end{cases} \tag{22}$$

with

$$f_a(\xi = \cos(\phi)) \equiv \frac{1}{2}[f_{\uparrow\uparrow}(|\boldsymbol{k} - \boldsymbol{q}|) - f_{\uparrow\downarrow}(|\boldsymbol{k} - \boldsymbol{q}|)]_{|\boldsymbol{k}|=|\boldsymbol{q}|=k_{\text{F}}} \tag{23}$$

(ϕ denotes the angle between $\boldsymbol{k}$ and $\boldsymbol{q}$).

We now address the question of which of the two ways of constructing the modified Hubbard fields accounts best for the many-body aspects of the system. For both methods one needs information on the spin stiffness $\partial^2\varepsilon_{\text{xc}}/\partial\zeta^2|_{\zeta=0}$, or, equivalently, the magnetic susceptibility χ_{M}. However, the information on $\varepsilon_{\text{xc}}(\zeta)$ is somewhat inconsistent.

For 3D the suggestion given by von Barth and Hedin [45] was shown to be a poor approximation by Vosko *et al* [36], who gave a fit for the deviation of the spin stiffness $\alpha_c(r_s)$ from its RPA value. Later, Perdew and Wang [46] determined a different Padé interpolation for $\alpha_c(r_s)$. In contrast to another suggestion by Perdew and Zunger [47], both forms are compatible with the recent simulations of reference [4]; the data, however, are insufficient for determining $\alpha_c(r_s)$ with confidence. Finally, Tanaka and Ichimaru [48] assume an *ansatz* for ε_{xc} with powers up to ζ^6; from the energy values obtained for a substantial number of ζ-values in the modified convolution approximation ('MCA'), they derived another Padé interpolation for $\alpha_c(r_s)$. For the 2D system, Tanatar and Ceperley [35] use a simple form that is quadratic in ζ for *either* the correlation *or* the full energy per particle. Due to the lack of a sufficient number of MC results at intermediate values of ζ, it appears difficult to decide which of the above is the most appropriate suggestion.

In order to circumvent these uncertainties, Yarlagadda and Giuliani [23] determined χ_{M} by means of a self-consistent calculation of m^* and g^*. We follow their suggestion by starting from either of the expressions (19) and (20), and fix three of the four parameters from the known values of $g(0)$ and κ. The remaining unknown

$$1/B_- = [1/B_{\uparrow\uparrow} - 1/B_{\uparrow\downarrow}]$$

is determined self-consistently, with the use of equations (16) and (18).

Figure 6 shows the resulting inverse magnetic susceptibility in comparison with the values discussed above. It is seen that $\chi_{\text{M}}^0/\chi_{\text{M}}$ approaches zero quite rapidly in the YG approximation—namely, at $r_s \approx 10$ and 4 in the 3D and 2D cases, respectively. In contrast, the IP parametrization is stable up to $r_s \approx 20$ and 9 (again for 3D and 2D). The IP curves are also much closer to the MC ones. Thus this parametrization appears superior to that of YG. Our data have been obtained with the use of the 'Ek' mass; the on-shell results lie significantly

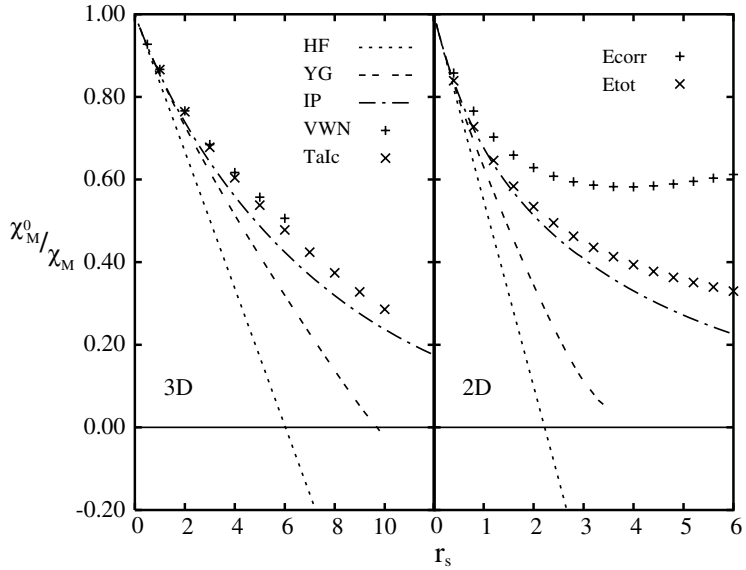

Figure 6. Inverse magnetic susceptibility. Dotted curve: the Hartree–Fock result. Symbols: MC (from reference [36] for 3D and reference [35] for 2D) and MCA results [48]. The double-dashed line was obtained with the Yarlagadda–Giuliani modified Hubbard form, equation (20), and the dashed–dotted one with that of Iwamoto and Pines, equation (19).

lower. For the 2D YG this latter choice limits the applicability range to $r_s \lesssim 3$. Though this range of values may be sufficient to cover the experiment of Fang and Stiles (see [16–18]), it is not acceptable for a description of the full density region that can be realized experimentally.

The vanishing of χ^0_M/χ_M corresponds to a divergence of g^*, where the self-consistency cycle becomes unstable. Our g^*-results are shown in figure 7 (to the best of our knowledge this is the first calculation of the Landé factor for the 3D system). We show the values obtained with either the YG or IP parametrization, calculated self-consistently or with the use of the best available results for the spin stiffness. Since we do not have reliable MC data beyond $r_s = 6$ in the 3D case, we used the MCA-based fit of reference [48] (which is very close to the VWN data, as seen in figure 6). For 2D we took the results derived from $\varepsilon_{\rm tot}$ by Tanatar and Ceperley [35]. There is little difference between the self-consistent and the literature-based YG predictions for g^*, its divergence at rather small r_s being clearly visible. For the IP case the self-consistent procedure yields more reasonable values than that using the MCA- and MC-based χ_M. Although these data for χ^0_M/χ_M remain positive up to $r_s \approx 19$ (the 3D MCA) and beyond $r_s = 40$ (the 2D MC), respectively, g^* computed from them diverges at much smaller values (correspondingly, equation (18) is grossly violated).

The symmetric fields $\mathcal{G}_+$ show little difference for YG and IP parametrizations. The anti-symmetrized local field $\mathcal{G}_-$ is shown in figure 8 for $r_s = 2$, together with MC simulation data given by Senatore *et al* [3]. It is seen that the IP *ansatz* allows for more structure and agrees better with the MC points, although its peak appears rather too low.

The values obtained for the effective mass are compared in figure 9 with those calculated without spin fluctuations. Obviously, the agreement with the reference data of Krotscheck [7] and Kwon *et al* [5] has become much poorer, the discrepancy being more pronounced in the 2D case. In contrast to the above findings, the 3D YG results are somewhat better than the IP results; for 2D neither curve is very satisfactory.

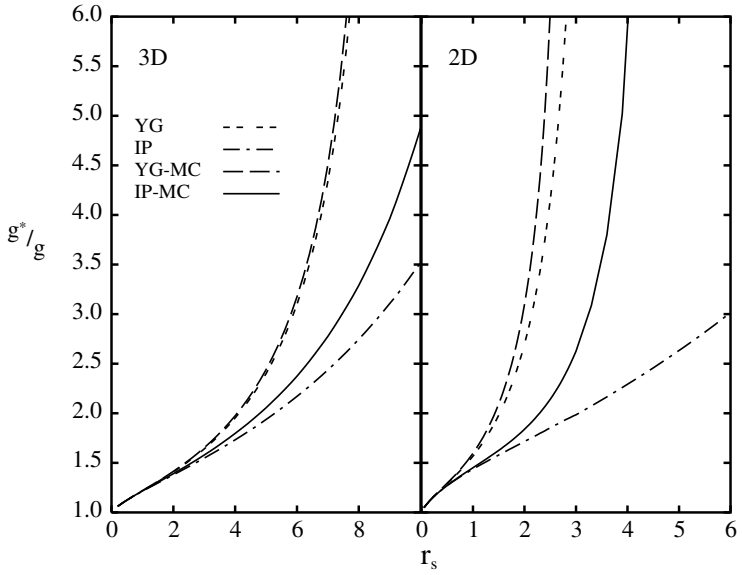

Figure 7. The Landé factor calculated with the YG (equation (20)) and IP (equation (19)) local field corrections. Double-dashed line: self-consistent YG result; long-dashed line: YG result with B_- from MCA [48] (3D) and MC simulation [35] (2D); dashed–dotted line: self-consistent IP result; solid line: MCA- and MC-based IP results.

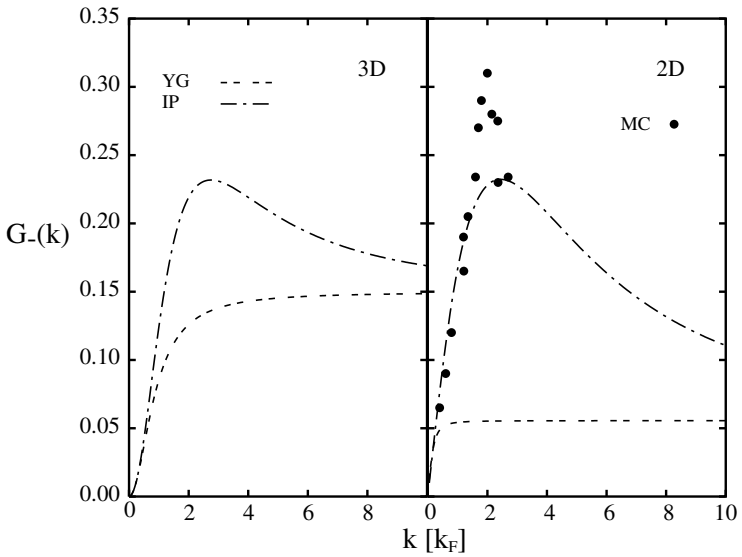

Figure 8. Local fields G_- for $r_s = 2$ in the self-consistent YG and IP approaches. The notation is the same as for figure 7; the full circles denote 2D MC results [3].

8. MOS layer

We now compare the IP and YG results for the more realistic case of a MOSFET, for which experimental values [16–18] are available. All relevant expressions are given in reference [23];

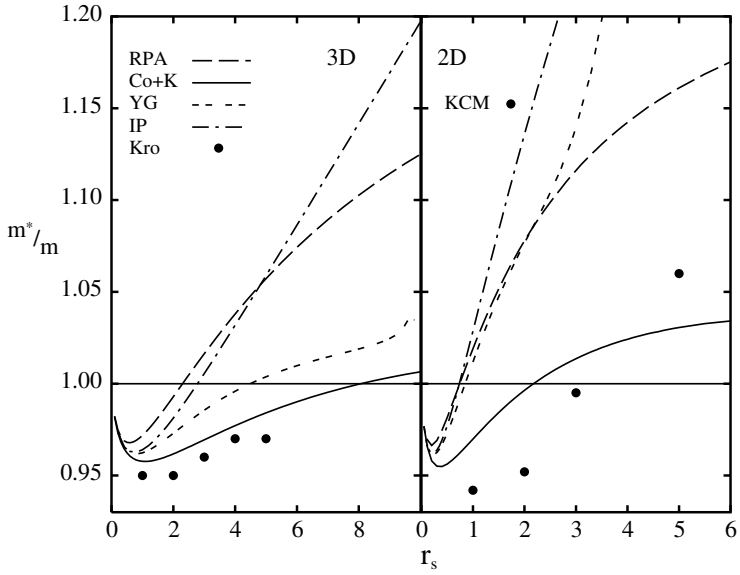

Figure 9. The effective mass including both charge and spin fluctuations. The double-dashed and dashed–dotted lines were calculated using the self-consistent YG and IP approaches, respectively. For comparison, the RPA results (long-dashed line) and the results without spin fluctuations (solid line) are shown. The symbols have the same meaning as for figure 2.

the extension of the wave function and the presence of the metallic gate are included via an overall form factor in front of the Coulomb interaction and in the local fields. The degeneracy $n_v = 2$ of the conduction band valley is also considered.

Figure 10 shows the comparison of the observables obtained with the two choices of approach: IP and YG. For m^*, both curves lie below the experimental results with the IP values being marginally closer than the YG values. The use of the on-shell mass (not shown) shifts the YG results to the extent that they cross the experimental curve—an implausible behaviour since phonons also contribute to the experimental m^*. The agreement of the YG prediction with the experimental values for the Landé factor is striking, with the IP results also lying acceptably close. The comparison with the experiment thus does not favour either of the two possibilities.

9. Summary

The results for m^* are dominated by the $k \to 0$ limit of the effective interaction, which is determined by the compressibility and is thus a macroscopic quantity. By using the best local fields available at present, constructed from state-of-the-art MC calculations for either $\omega = 0$ or from $S(k)$, we demonstrated the necessity for a consistent treatment of the vertex. This can be achieved by replacing the interaction v/ϵ in the G^0W-approach with the mean particle–particle potential. By comparing the full leading-order exchange contribution with that of the Hubbard approximation, we showed that the underlying localization is justified. When only charge fluctuations are accounted for in the calculations, the use of our MC-based local field corrections gives a very close agreement of m^* with available benchmark results in the 3D case and a satisfactory one for 2D. We further found that approximating the local fields by a modified Hubbard form fulfilling the compressibility sum rule and Kimball's sum rules still

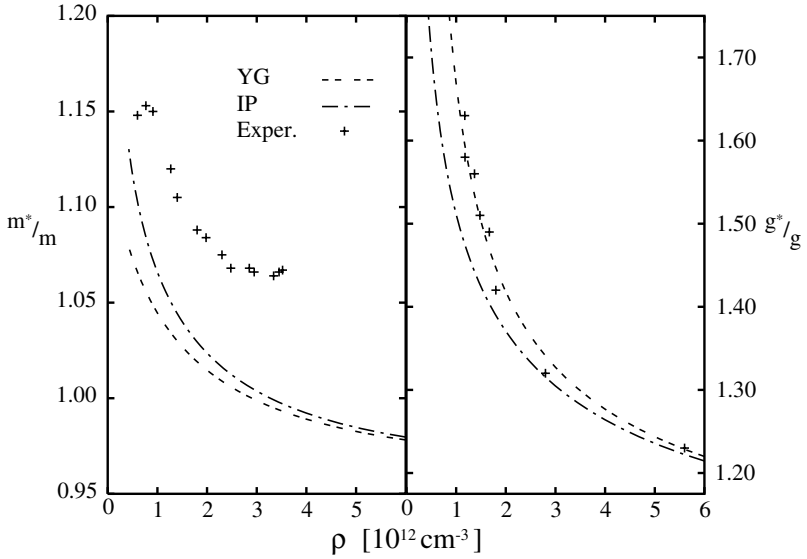

Figure 10. The effective mass (left) and the Landé factor (right) for the MOS structure in terms of the electron density. Compared are the self-consistent YG (double-dashed line) and IP (dashed–dotted line) approaches; also shown are the experimental results of Fang and Stiles (see [16–18]).

yields good results for m^*. This is of importance, since applications to realistic systems usually lack the (MC) information available for jellium.

Spin fluctuations formally enter the effective interaction via the local field factor $\mathcal{G}_-$. Due to the lack of suitable information from simulations for the spin quantities, one is restricted to simple parametrizations; we chose again a modified Hubbard form. The question of whether this *ansatz* is better made for the partial functions $\mathcal{G}_{\uparrow\uparrow(\downarrow)}$ as introduced by Iwamoto and Pines [42] or directly for $\mathcal{G}_\pm$ as suggested later by Yarlagadda and Giuliani [23] cannot be decided unambiguously. We found the IP method to be superior as regards self-consistent results for the magnetic susceptibility χ_M (and, correspondingly, $\mathcal{G}_-(k \to 0)$), with respect to the range of applicability of the approach (limited by the fact that the self-consistent procedure becomes unstable where $1/\chi_M$ vanishes), and also as regards the shape of $\mathcal{G}_-$. On the other hand, the YG choice yields somewhat better data for the effective mass. The application of the formalism to a Si–SiO_2 MOSFET gives a reasonable agreement of the YP as well as the IP results with the experimental data [16–18].

In general it can be stated that the IP *ansatz* allows for more structure in the local field factors. Further information concerning this point from MC calculations for $\mathcal{G}_-$ at various r_s-values would be highly desirable. Also, a better knowledge of the spin stiffness from simulation studies appears necessary. As a final remark, we note the following: Krakovsky and Percus [15] report m^* to be a *decreasing* function of r_s in the 3D case, whereas it *increases* for 2D. This is in contrast to our findings, where the same type of approach always yields similar r_s-behaviours for 3D and 2D.

Acknowledgment

The work was supported, in part, by the Austrian Science Fund under project P11098-PHY.

References

[1] Moroni S, Ceperley D M and Senatore G 1992 *Phys. Rev. Lett.* **69** 1837
[2] Moroni S, Ceperley D M and Senatore G 1995 *Phys. Rev. Lett.* **75** 689
[3] Senatore G, Moroni S and Ceperley D M 1998 *Quantum Monte Carlo Methods in Physics and Chemistry (NATO ASI Series)* ed P Nightingale and C Umrigar (Dordrecht: Kluwer)
[4] Ortiz G and Ballone P 1994 *Phys. Rev.* B **50** 1391
[5] Kwon Y, Ceperley D M and Martin R M 1994 *Phys. Rev.* B **50** 1684
[6] Rapisarda F and Senatore G 1996 *Aust. J. Phys.* **49** 161
[7] Krotscheck E 1984 *Ann. Phys., NY* **155** 1
[8] Kukkonen C A and Overhauser A W 1979 *Phys. Rev.* B **20** 550
[9] Vignale G and Singwi K S 1985 *Phys. Rev.* B **32** 2156
[10] Ng T K and Singwi K S 1986 *Phys. Rev.* B **34** 7738
Ng T K and Singwi K S 1986 *Phys. Rev.* B **34** 7743
[11] Zhu X and Overhauser A W 1986 *Phys. Rev.* B **33** 925
[12] Yasuhara H and Takada Y 1991 *Phys. Rev.* B **43** 7200
[13] Yasuhara H and Ousaka Y 1992 *Int. J. Mod. Phys.* B **6** 3089
[14] Nakano A and Ichimaru S 1989 *Phys. Rev.* B **39** 4938
[15] Krakovsky A and Percus J 1996 *Phys. Rev.* B **53** 7352
[16] Fang F F and Stiles P J 1968 *Phys. Rev.* **174** 823
[17] Smith J L and Stiles P J 1972 *Phys. Rev. Lett.* **29** 102
[18] Fang F F, Fowler A B and Hartstein A 1977 *Phys. Rev.* B **16** 4446
[19] Suzuki K and Kawamoto Y 1973 *J. Phys. Soc. Japan* **35** 1456
[20] Vinter B 1976 *Phys. Rev.* B **13** 4447
[21] Lee T K, Ting C S and Quinn J J 1975 *Phys. Rev. Lett.* **35** 1048
[22] Lee T K, Ting C S and Quinn J J 1976 *Surf. Sci.* **58** 246 and references therein
[23] Yarlagadda S and Giuliani G F 1990 *Surf. Sci.* **229** 410
[24] Yarlagadda S and Giuliani G F 1994 *Phys. Rev.* B **49** 14 188 and references therein
[25] Mamorkos I K and Sarma S D 1991 *Phys. Rev.* B **44** 3451
[26] Jang Y R and Min B I 1993 *Phys. Rev.* B **48** 1914
[27] Lindhard J 1954 *K. Danske Vidensk. Selsk. Mat.-Fys. Meddr.* **8** 28
[28] Stern F 1967 *Phys. Rev. Lett.* **18** 546
[29] Hubbard J 1957 *Proc. R. Soc.* A **243** 336
[30] Pines D and Nozières P 1966 *The Theory of Quantum Liquids* vol I (New York: Benjamin)
[31] Rice T M 1965 *Ann. Phys., NY* **31** 100
[32] Kimball J C 1973 *Phys. Rev.* A **7** 1648
[33] Rajagopal A K and Kimball J C 1977 *Phys. Rev.* B **15** 2819
[34] Holas A 1986 *Strongly Coupled Plasma Physics* ed F J Rogers and H E DeWitt (New York: Plenum) pp 463–82
[35] Tanatar B and Ceperley D M 1989 *Phys. Rev.* B **39** 5005
[36] Vosko S H, Wilk L and Nusair M 1980 *Can. J. Phys.* **58** 1200
[37] Yasuhara H 1974 *J. Phys. Soc. Japan* **36** 361
[38] Isawa Y and Yasuhara H 1983 *Solid State Commun.* **46** 807
[39] Rapisarda F, private communication
[40] Rietschel H and Sham L J 1983 *Phys. Rev.* B **28** 5100
[41] Santoro G E and Giuliani G F 1988 *Phys. Rev.* B **37** 4813
[42] Iwamoto N and Pines D 1984 *Phys. Rev.* B **29** 3924
[43] Iwamoto N 1991 *Phys. Rev.* B **43** 2174
[44] Janak J F 1969 *Phys. Rev.* **178** 1416
[45] von Barth U and Hedin L 1972 *J. Phys. C: Solid State Phys.* **5** 1629
[46] Perdew J P and Wang Y 1992 *Phys. Rev.* B **45** 13 244
[47] Perdew J P and Zunger A 1981 *Phys. Rev.* B **23** 5048
[48] Tanaka S and Ichimaru S 1989 *Phys. Rev.* B **39** 1036